A Letters Journal Exploring the Frontiers of Physics

September 2014

EPL, **107** (2014) 68005
doi: 10.1209/0295-5075/107/68005

www.epljournal.org

Reconstructing neural dynamics using data assimilation with multiple models

Franz Hamilton, John Cressman, Nathalia Peixoto and Timothy Sauer

George Mason University - Fairfax, VA, USA

received 29 July 2014; accepted in final form 5 September 2014
published online 19 September 2014

PACS 87.19.L- – Neuroscience
PACS 05.45.Tp – Time series analysis
PACS 07.05.Kf – Data analysis: algorithms and implementation; data management

Abstract – Assimilation of data with models of physical processes is a critical component of modern scientific analysis. In recent years, nonlinear versions of Kalman filtering have been developed, in addition to methods that estimate model parameters in parallel with the system state. We propose a substantial extension of these tools to deal with the specific case of unmodeled variables, when training data from the variable is avaiable. The method uses a stack of several, nonidentical copies of a physical model to jointly reconstruct the variable in question. We demonstrate the ability of this technique to accurately recover an unmodeled experimental quantity, such as an ion concentration, from a single voltage trace after the training period is completed. The method is applied to reconstruct the potassium concentration in a neural culture from multielectrode array voltage measurements.

Modern data-assisted modeling in the physical and biological sciences depends heavily on the use of data assimilation techniques to fit unobserved model variables. Their use in the case of nonlinear models has become standard in numerical weather prediction [1–4], oceanography [5], and various areas of spatiotemporal dynamics [6–9]. In the nonlinear case, the Extended Kalman Filter (EKF) and Ensemble Kalman Filter (EnKF) have become routine.

Standard extensions of this methodology are used to approximate model parameters, in addition to unobserved variables of the model. This approach, known as dual estimation [10–13], essentially treats system parameters as slowly evolving variables. Recently, implementations using the dual ensemble Kalman filter have been used for parameter estimation in various neuroscience experiments [14–16]. Of course, the above-mentioned approaches are limited to reconstructing state variables and parameters that are explicitly represented in the model.

In this letter we show how this general methodology can be naturally extended further, to reconstruct variables of the system that do not appear in the model, but for which limited time series measurements are available. A result of Takens [17–20] shows that sufficiently generic time series measurements can be used to reconstruct system dynamics. This knowledge has been long used as a basis for black-box prediction, noise reduction, and control protocols for nonlinear systems. Here we take a first step at merging this powerful theory with modern methods of data analysis that can exploit information from models.

The basic concept involves assimilating the available time series in parallel with multiple, different versions of the model. In our examples, we use a single model under a variety of fixed parameter settings. During a training period, data from both modeled variables and the unmodeled variable are available, and a parameterized combination of reconstructed model variables is fit to the unmodeled variable. After the training period, this combination is used to track the unmodeled variable. An arbitrary number of unmodeled variables can be tracked simultaneously and independently with this method.

Our approach essentially merges two lines of research on modeling and predicting behavior of nonlinear systems. One direction, motivated by the seminal paper by Lorenz [21], attempts to build a collection of models with slightly different parameters, and regress during a training period on the outputs of the models of a particular variable to build a good predictor for that variable [22,23]. Independently, researchers in data assimilation have used multimodel versions of the Kalman filter [24] and the EnKF [25–27] to improve the tracking capability of the modeled variables. Our approach combines the ideas by training a multimodel EnKF on some known time series

data from a variable that is not included in the underlying model, and using the fitted result to predict the unmodeled variable after the training period ends. We think of the approach as a "platypus" method, since our basic ansatz is that the unmodeled variable is a combination of nominally unrelated parts.

A further advantage of a data assimilation approach to the problem is that after the training period, the unmodeled variable can be computed in real time. Moreover, if further training data becomes subsequently available, it can be easily exploited to further refine the parameterized combination, or to do real-time tracking under circumstances of drifting parameters.

To illustrate the idea, let us assume the system model

$$\begin{aligned} \dot{x} &= f(x,p) + \omega_t, \\ y &= h(x) + \nu_t \end{aligned} \tag{1}$$

for state vector x and vector p of parameters. Here ω_t and ν_t are white-noise inputs. The function h is a vector-valued observation of the state. The standard filtering problem is to use the time series of observations y_t to calculate an estimate for the current state x.

The innovation of this method is to go beyond estimating unobserved variables and parameters in the model, *i.e.* the components of x and p, to estimate quantities that are not explicit model variables or parameters. We assume that a time series S_t of the desired unmodeled variable is available during a training phase, with the goal of continuing to estimate the variable after the training period has ended.

We construct a parallel set of m subfilters, each of which are the system model with separate parameter settings p_i. This parallel set is used for data assimilation during the *training phase*, corresponding to the equation

$$\begin{aligned} \dot{w} &= F(w) + \omega_t, \\ \begin{bmatrix} y \\ \vdots \\ y \\ S \end{bmatrix} &= H(w) + \nu_t, \end{aligned} \tag{2}$$

where

$$w = \begin{bmatrix} x^1 \\ \vdots \\ x^m \\ c^1 \\ \vdots \\ c^m \\ d \end{bmatrix}, \quad F = \begin{bmatrix} f(x,p_1) \\ \vdots \\ f(x,p_m) \\ 0 \\ \vdots \\ 0 \\ 0 \end{bmatrix},$$

$$H(w) = \begin{bmatrix} h(x^1) \\ \vdots \\ h(x^m) \\ \sum_{i,j} c_j^i x_j^i + d \end{bmatrix}.$$

Note that each x^i denotes a separate copy of the system state vector, with n components x_j^i for $j = 1, \ldots, n$. Each c^i is an unknown coefficient vector of n components c_j^i that will be learned along with the states x^i during the assimilation process, in order to best fit the unmodeled variable $S = \sum_{i,j} c_j^i x_j^i + d$. The inputs to the assimilation procedure during the training phase are the modeled observables y_t, and the time series S_t of the unmodeled variable, that is provided only during the training phase. The coefficients c_j^i and d are estimated during the training phase (along with the system variables x_j^i), and then fixed during the *prediction phase*, which uses only the y_t inputs, and assimilates the system model

$$\begin{aligned} \dot{w} &= F(w), \\ \begin{bmatrix} y \\ \vdots \\ y \end{bmatrix} &= H(w), \end{aligned} \tag{3}$$

where

$$w = \begin{bmatrix} x^1 \\ \vdots \\ x^m \end{bmatrix}, \quad F = \begin{bmatrix} f(x,p_1) \\ \vdots \\ f(x,p_m) \end{bmatrix},$$

$$H(w) = \begin{bmatrix} h(x^1) \\ \vdots \\ h(x^m) \end{bmatrix}.$$

During the prediction phase, the expression $\sum_{i,j} c_j^i x_j^i + d$ gives an estimate of the unmodeled quantity S using only the y_t inputs.

For nonlinear models, the assimilation can be done using dual versions of either the EKF or the EnKF; we use the latter in the following results. Equations for the EnKF are given in appendix A.

As a simple demonstration, we describe the reconstruction of a gating variable from the Hodgkin-Huxley (HH) neural model [28] consisting of four differential equations, modeling the voltage V and three gating variables h, m and n (see the first subsection of appendix B). We will use the Hodgkin-Huxley equations to generate a time series of the four variables. However, for the purposes of the illustration, we make no use of the knowledge of how the time series was created. As the assimilation model, we purposely choose an unrelated, standard spiking model,

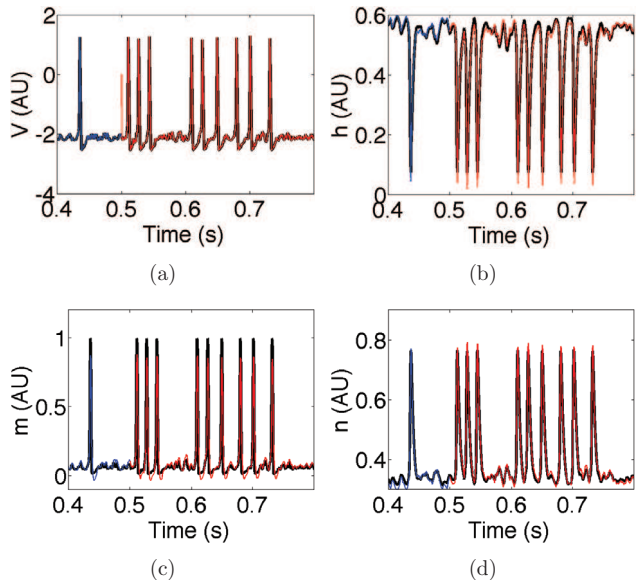

Fig. 1: (Color online) Estimating unmodeled dynamics using data assimilation with multiple models. Hodgkin-Huxley time series is input into the EnKF using Hindmarsh-Rose multiple models. The end of the training phase and beginning of the prediction phase are shown. (a) Hodgkin-Huxley voltage (black) and assimilated version of voltage in training phase (blue) and prediction phase (red). (b) Hodgkin-Huxley gating variable h (black) and assimilated version of h. During the prediction phase (red), only the Hodgkin-Huxley voltage is available to the EnKF. The procedure also obtains the other two Hodgkin-Huxley gating variables, (c) m and (d) n.

the Hindmarsh-Rose (HR) equations [29]

$$\begin{aligned} \dot{V} &= y - V^3 + 3V^2 - z + I, \\ \dot{y} &= 1 - bV^2 - y, \\ \dot{z} &= \tau(s(V+1) - z), \end{aligned} \tag{4}$$

where V represents the voltage, y is a fast recovery variable and z is a slow variable. The rate of z is controlled by the time scale parameter τ, while I, b and s are free parameters to be estimated alongside the state variables V, y and z by the EnKF [13,14,16,30]. We use $V(t)$ and $h(t)$ from the Hodgkin-Huxley series during the training phase. Note that 1) the gating variable $h(t)$ is not explicitly represented as a variable in the assimilation model (the Hindmarsh-Rose equations) and is therefore an unmodeled dynamic, and 2) the waveforms of HR (see fig. 2(b) for an example) are quite unlike all waveforms of the HH variables (see fig. 1(a)–(d)).

In the assimilation process, we use two HR models to reconstruct $h(t)$, with time scale parameters $\tau_1 = 0.001$ and $\tau_2 = 0.1$, respectively. According to (2), we make the approximation $h(t) \approx \sum_{i,j} c_j^i x_j^i + d$. Using two assimilation models, this approximation during the training phase can be achieved in several ways. If we reconstruct using only the y variables from the models, we find $h(t) \approx -2.46y_1 + 1.92y_2 + 0.50$ as a result of the training phase. This approximation gives us prediction root mean squared error (RMSE) = 0.140. A much improved reconstruction uses only the z variables, giving the approximation $h(t) \approx 1.21z_1 - 0.17z_2 - 1.35$ which yields prediction RMSE = 0.025. Using both the y and z variables yields the most accurate estimate $h(t) \approx -0.42y_1 + 0.33z_1 + 0.48y_2 - 0.16z_2 - 0.83$, and prediction RMSE = 0.016, as shown in fig. 1(b). When it is unknown *a priori* which variables allow for a more faithful reconstruction of the unmodeled quantity, all variables can be considered for discovery of the optimal weighting. We repeat this process and reconstruct the $m(t)$ and $n(t)$ gating variables, shown in fig. 1(c), (d), using two assimilation models each.

To further simulate the type of model error we would encounter in a laboratory setting, we consider data generated from a second, more sophisticated system as described in [31], where it was used to investigate ionically mediated bursting. The model equations (see the second subsection of appendix B) include the membrane potential based on transmembrane currents for sodium and potassium. The gating variables for potassium activation and sodium inactivation are modeled dynamically whereas the sodium activation is assumed to be instantaneous. In addition, the ionic dynamics for extracellular and intracellular potassium and sodium concentrations, respectively, are modeled by two equations. Sodium concentrations depend only on transmembrane conductances making their intra- and extracellular concentrations linked through mass conservation. The extracellular potassium dynamics also include glial buffering.

The model was driven by a Poisson spike train to create a sequence of irregular seizures, shown in fig. 2(a). As with the HH data from our first example, the potential is treated as the observable of the system. The goal is to use data assimilation with the (unrelated) HR model to reconstruct and predict the sodium and potassium concentrations, given only the voltage and a brief sequence of training data. The increased complexity of these data requires us to use three copies of the HR model. We set two of the models to have time scale parameters $\tau_1 = 0.001$ and $\tau_2 = 0.0001$ and individually optimize the third time scale, τ_3, for minimum training phase RMSE. Figure 2 shows the resulting reconstruction of the potassium and sodium dynamics from this system. Using only three assimilation models we are able to reconstruct these quantities with a high degree of accuracy (RMSE = 0.12 and 0.11, respectively).

To apply the method in a laboratory setting, we collected a potassium time series from a neural culture experiment. Cortical neurons extracted from embryonic day 17 mice were cultured on microelectrode arrays as described in [32]. A microelectrode array (MEA) provides a convenient *in vitro* platform for the study of neuronal networks by allowing for the simultaneous recording of the neuronal extracellular potential at each of the array's electrodes. Cultures were kept in incubator under controlled temperature (37 °C) and humidity (10% CO_2)

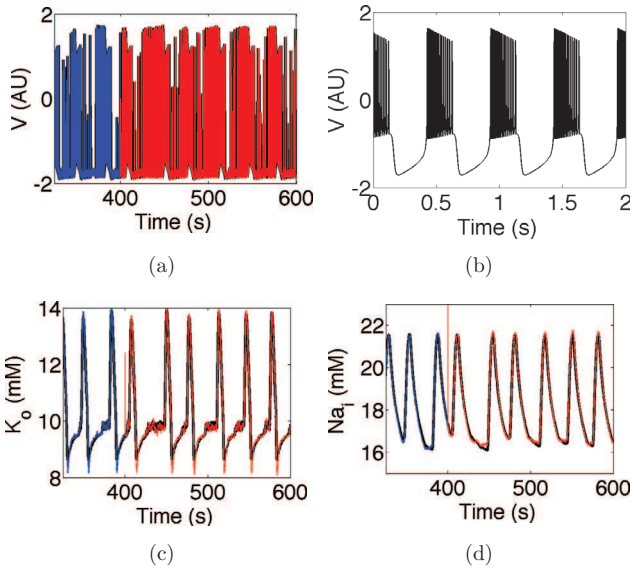

Fig. 2: (Color online) Estimation and prediction of simulated seizure dynamics. A single seizing neuron is driven by a Poisson spike train with constant parameter λ. The neuron voltage (a) is continuously measured, and assimilated using the EnKF with three versions of HR, whose voltage trace is shown in (b) with parameters $b = 5, \tau = 0.001, s = 4$ and $I = 0$. Potassium (c) and sodium (d) are only observed for a brief training period of 200 s. During the training period, our algorithm finds the optimal combination of the model variables (blue). After this training period, we can predict (red) the potassium (RMSE = 0.12) and sodium (RMSE = 0.11) dynamics from the three HR models.

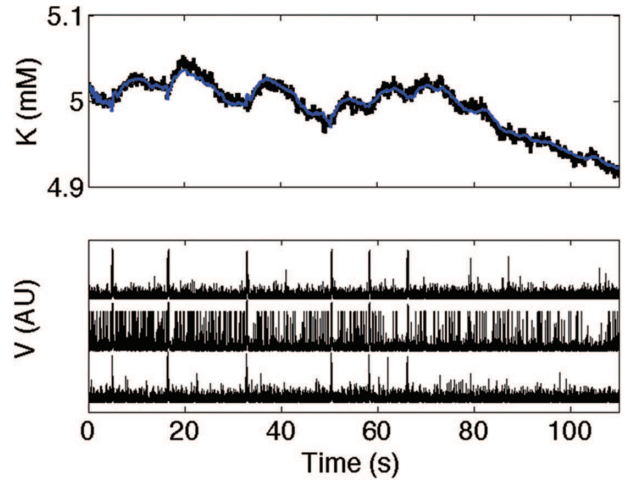

Fig. 3: (Color online) Training phase for potassium measurements. A potassium-sensitive electrode is used to record the extracellular potassium concentration changes in a small region between three active electrodes of an *in vitro* cortical culture plated on an MEA. During a 110 s training period, the potential from the three electrodes is assimilated and estimated with our EnKF (bottom), while an optimal combination of the model variables is found (top, blue) to reconstruct the measured potassium (top, black). For this example, each electrode is represented by four differently parameterized models, resulting in a total of twelve system models.

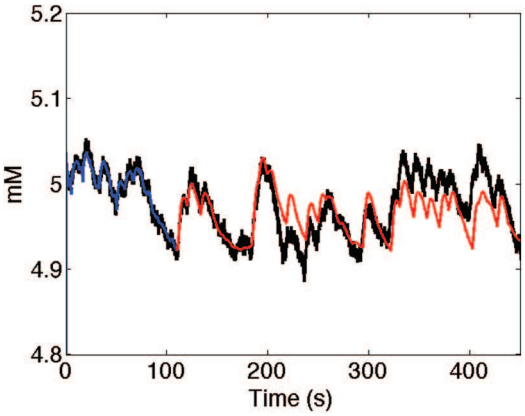

Fig. 4: (Color online) Training and prediction phases for potassium measurements. After the training period is complete, eq. (3) accurately predicts (RMSE = 0.024) the potassium concentration changes during spontaneous activity while using as input only the neural potential from 3 MEA electrodes.

until recording at 28 days *in vitro*. Extracellular recordings were obtained with a Multichannel Systems (MCS) recording system (Reutlingen, Germany) and temperature was maintained at 37 °C with a heated baseplate. Each electrode was recorded at a rate of 25 kHz, but downsampled to 1 kHz. Individual units on active electrodes were not sorted, meaning each electrode was considered as a neural assembly. The recorded time series from each electrode was filtered and rectified prior to assimilation.

Local potassium measurements were performed using the same type of resin-based potassium-sensitive microelectrodes used in slice experiments [33]. Potassium and reference electrodes are positioned in the mat of cultured cells located in the vicinity of a three active MEA recording sites. The potassium data are acquired using an high-impedance differential amplifier and digitized and recorded at 100 Hz. The data are low-pass filtered and input to the Nernst equation to find to potassium concentration in the vicinity of the electrode.

Figure 3 shows the recorded *in vitro* neural activity from each of the three electrodes during the training phase. The assimilation is done with eq. (2) using four HR models for each electrode, with time scales $\tau_1 = 0.001, \tau_2 = 0.0001, \tau_3 = 0.005, \tau_4 = 0.0005$, resulting in a total of twelve system models. Here the training period is only 110 seconds, during which the potassium and potential are available for assimilation and an optimal weighting of the twelve models is found to reconstruct the potassium time series. Figure 4 shows the prediction phase, where we are able to track the potassium dynamics while only assimilating the neural potential. Discrepancy between the actual and predicted values may be partially attributed to uncertainties in our measurement, since the potassium is recorded from a general region rather than a specific cell and there are likely other active neurons in the area, contributing to the potassium changes whose potential we are unable to capture due to the MEA architecture.

We have introduced an extension of standard data assimilation techniques, based on Takens' embedding theorem, that uses a short time series from an unmodeled variable to train a predictor for the variable using multiple versions of the model. The use of multiple versions serves to bring the strength of relatively simple mathematical modeling to bear on complicated dynamics, by training with time series data. For simplicity, we described an implementation with the EnKF, and used the Hindmarsh-Rose equations as a basic model, even though the latter is designed for intracellular, not extracellular dynamics. With appropriate modifications, other data assimilation techniques, and other models, can be readily substituted.

The approach taken here is global in the sense that the coefficients c_j^i are constant in phase space. To the extent that the data makes it practical, it may be beneficial to develop a further extension of these ideas that treats the data more locally.

Although we demonstrate its use for variables that do not appear in the model, the method can be beneficial in cases of poorly modeled variables, or in general when the model error is significant. The success of the method will depend on the choice of the multiple models. We have found that the method works well when using neural models to reconstruct quantities that are not included among the model variables. Its use will be crucial for experiments on control of spreading depression and seizures in neural cultures, where extensive, real-time measurements of potassium and calcium concentrations are needed but are not feasible, while voltages are easily available. We expect the method to find application in a variety of physics, geophysics and biological contexts where current models are poor or nonexistent.

* * *

The research was partially supported by grants CMMI-1300007, DMS-1216568 and DMS-1250936 from the National Science Foundation. We thank Tyrus Berry for helpful comments.

Appendix A. Data assimilation equations: the EnKF. – In our data assimilation we assume a general nonlinear system with n-dimensional state vector x and m-dimensional observation vector y defined by

$$\begin{aligned} x_{k+1} &= f(x_k, t_k) + w_k, \\ y_k &= h(x_k, t_k) + v_k, \end{aligned} \tag{A.1}$$

where w_k and v_k are white noise with covariance matrices Q and R, respectively. The ensemble Kalman filter (EnKF) approximates a nonlinear system using a weighted ensemble. The filter is initialized with state vector $x_0^+ = 0_{n\times 1}$ and covariance matrix $P_0^+ = I_{n\times n}$. At the k-th step of the filter there is an estimate of the state x_{k-1}^+ and the covariance matrix P_{k-1}^+.

The singular value decomposition is used to find the symmetric positive definite square root S_{k-1}^+ of the matrix P_{k-1}^+. We use the scaled unscented transformation (see, for example, [34]) to form a weighted ensemble of state vectors. The model f is applied to this ensemble, advancing it one time step, and then observed with function h. The mean of the resulting state ensemble gives the *a priori* state estimate x_k^- and the mean of the observed ensemble is the predicted observation y_k^-. Denoting the covariance matrices P_k^- and P_k^y of the resulting state and observed ensemble, and the cross-covariance matrix P_k^{xy} between the state and observed ensembles, the equations

$$\begin{aligned} K_k &= P_k^{xy}(P_k^y)^{-1}, \\ P_k^+ &= P_k^- - P_k^{xy}(P_k^y)^{-1}P_k^{yx}, \\ x_k^+ &= x_k^- + K_k\left(y_k - y_k^-\right) \end{aligned} \tag{A.2}$$

are used to update the state and covariance estimates with the observation y_k.

Appendix B. Neuron models. –

Hodgkin-Huxley model [28]. The Hodgkin-Huxley equations form a system of four ordinary differential equations,

$$\begin{aligned} C\frac{\mathrm{d}V}{\mathrm{d}t} &= -g_1 m^3 h(V-E_1) - g_2 n^4(V-E_2) \\ &\quad - g_3(V-E_3) + I_{\mathrm{stim}}, \\ \frac{\mathrm{d}m}{\mathrm{d}t} &= (1-m)\alpha_m(V-E_0) - m\beta_m(V-E_0), \\ \frac{\mathrm{d}n}{\mathrm{d}t} &= (1-n)\alpha_n(V-E_0) - n\beta_n(V-E_0), \\ \frac{\mathrm{d}h}{\mathrm{d}t} &= (1-h)\alpha_h(V-E_0) - h\beta_h(V-E_0), \end{aligned}$$

where

$$\begin{aligned} \alpha_m(V) &= \frac{2.5-0.1V}{\exp(2.5-0.1V)-1}, \quad \beta_m(V) = 4\exp\left(-\frac{V}{18}\right), \\ \alpha_n(V) &= \frac{0.1-0.01V}{\exp(1-0.1V)-1}, \quad \beta_n(V) = \frac{1}{8}\exp\left(-\frac{V}{80}\right), \\ \alpha_h(V) &= 0.07\exp\left(-\frac{V}{20}\right), \quad \beta_h(V) = \frac{1}{\exp(3-0.1V)+1}. \end{aligned}$$

The parameters of the system are set to typical values: $C = 1, E_0 = -65, E_1 = 50, E_2 = -77, E_3 = -54.4$, and I_{stim} is a stimulating Poisson spike train with parameter λ.

Model of ionically mediated bursting [31]. The model consists of five differential equations,

$$\begin{aligned} C\frac{\mathrm{d}V}{\mathrm{d}t} &= -I_{\mathrm{Na}} - I_{\mathrm{K}} - I_{\mathrm{Cl}} + I_{\mathrm{stim}}, \\ \tau\frac{\mathrm{d}[\mathrm{K}]_o}{\mathrm{d}t} &= \gamma\beta(I_{\mathrm{K}} - 2I_{\mathrm{pump}}) - \tilde{I}_{\mathrm{glia}} - \tilde{I}_{\mathrm{diffusion}}, \\ \tau\frac{\mathrm{d}[\mathrm{Na}]_i}{\mathrm{d}t} &= -\gamma(I_{\mathrm{Na}} + 3I_{\mathrm{pump}}), \\ \frac{\mathrm{d}h}{\mathrm{d}t} &= \phi\left[\alpha_h(V)(1-h) - \beta_h(V)h\right], \\ \frac{\mathrm{d}n}{\mathrm{d}t} &= \phi\left[\alpha_n(V)(1-n) - \beta_n(V)n\right]. \end{aligned}$$

The first equation describes the spiking behavior where C is the membrane capacitance, V is the membrane potential, and the membrane ion current densities are defined as

$$\begin{aligned} I_{\mathrm{Na}} &= g_{\mathrm{Na}} m_{\infty}^{3} h\,(V - E_{\mathrm{Na}}) + g_{\mathrm{NaL}}\,(V - E_{\mathrm{Na}}), \\ I_{\mathrm{K}} &= g_{\mathrm{K}} n^{4}\,(V - E_{\mathrm{K}}) + g_{\mathrm{KL}}\,(V - E_{\mathrm{K}}), \\ I_{\mathrm{Cl}} &= g_{\mathrm{ClL}}\,(V - E_{\mathrm{Cl}}). \end{aligned}$$

I_{stim} is a stimulating Poisson spike train with parameter λ. The second and third differential equations model the time evolution of the local extracellular potassium and the intracellular sodium concentrations. In these equations the $\tilde{I}$'s are molar currents (millimolars per second) and depend on the ion concentrations as follows:

$$\begin{aligned} I_{\mathrm{p}} &= \frac{\rho}{\gamma}\left(\frac{1}{1+\exp\left(\frac{25.0-[\mathrm{Na}]_i}{3.0}\right)}\right) \\ &\quad \times \left(\frac{1}{1+\exp\left(5.5-[\mathrm{K}]_o\right)}\right), \\ \tilde{I}_{\mathrm{diff}} &= \varepsilon\left([\mathrm{K}]_o - [\mathrm{K}^{+}]_{\mathrm{bath}}\right), \\ \tilde{I}_{\mathrm{glia}} &= \frac{G_{\mathrm{glia}}}{1.0+\exp\left(\frac{18.0-[\mathrm{K}]_o}{2.5}\right)}. \end{aligned}$$

The fourth and fifth differential equations represent the gating variables where

$$\begin{aligned} \alpha_h(V) &= 0.07\exp\left(-\frac{V+44}{20}\right), \\ \beta_h(V) &= \frac{1}{1+\exp(-0.1(V+14))}, \\ \alpha_n(V) &= \frac{0.01(V+34)}{1-\exp(-0.1(V+34))}, \\ \beta_n(V) &= 0.125\exp\left(-\frac{V+44}{80}\right). \end{aligned}$$

For simplification, we follow [31] in making the assumption

$$\begin{aligned} [\mathrm{K}]_i &= 140.0\,\mathrm{mM} + (18.0\,\mathrm{mM} - [\mathrm{Na}]_i), \\ [\mathrm{Na}]_o &= 144.0\,\mathrm{mM} - \beta\,([\mathrm{Na}]_i - 18.0\,\mathrm{mM}) \end{aligned}$$

which allows us to define the sodium and potassium equilibrium potentials E_{Na} and E_K, respectively,

$$\begin{aligned} E_{\mathrm{K}} &= 26.64\ln\left(\tfrac{[\mathrm{K}]_o}{[\mathrm{K}]_i}\right), \\ E_{\mathrm{Na}} &= 26.64\ln\left(\tfrac{[\mathrm{Na}]_o}{[\mathrm{Na}]_i}\right). \end{aligned}$$

REFERENCES

[1] Kalnay E., *Atmospheric Modeling, Data Assimilation, and Predictability* (Cambridge University Press) 2003.

[2] Evensen G., *Data Assimilation: The Ensemble Kalman Filter* (Springer, Heidelberg) 2009.

[3] Rabier F., *Q. J. R. Meteorol. Soc.*, **131** (2005) 3215.

[4] Hunt B., Kalnay E. and Kostelich E., *Tellus A*, **56** (2004) 273.

[5] Cummings J. A., *Q. J. R. Meteorol. Soc.*, **131** (2005) 3583.

[6] Yoshida K., Yamaguchi J. and Kaneda Y., *Phys. Rev. Lett.*, **94** (2005) 014501.

[7] Law K. and Stuart A., *Mon. Weather Rev.*, **140** (2012) 3757.

[8] Schiff S., *Neural Control Engineering* (MIT Press) 2012.

[9] Berry T. and Sauer T., *Tellus A*, **65** (2013) 20331.

[10] Kopp R. and Orford R., *AIAA J.*, **1** (1963) 2300.

[11] Cox H., *IEEE Trans. Autom. Control*, **9** (1964) 5.

[12] Wan E. and Nelson A., in *Kalman Filtering and Neural Networks*, edited by Haykin S. (Wiley Interscience) 2001, p. 123.

[13] Voss H., Timmer J. and Kurths J., *Int. J. Bifurcat. Chaos*, **14** (2002) 1905.

[14] Ullah G. and Schiff S., *Phys. Rev. E*, **79** (2009) 040901.

[15] Sauer T. and Schiff S., *Phys. Rev. E*, **79** (2009) 051909.

[16] Ullah G. and Schiff S., *PLoS Comput. Biol.*, **6** (2010) e1000776.

[17] Takens F., *Lect. Notes Math.*, Vol. **898** (Springer-Verlag, Berlin) 1981.

[18] Packard N., Crutchfield J., Farmer D. and Shaw R., *Phys. Rev. Lett.*, **45** (1980) 712.

[19] Sauer T., Yorke J. and Casdagli M., *J. Stat. Phys.*, **65** (1991) 579.

[20] Sauer T., *Phys. Rev. Lett.*, **93** (2004) 198701.

[21] Lorenz E., *J. Atmos. Sci.*, **20** (1963) 130.

[22] Krishnamurti T., Kishtawal C. and Zhang Z., *Science*, **285** (1999) 1548.

[23] Krishnamurti T., Kishtawal C. and Zhang Z., *J. Clim.*, **13** (2000) 4196.

[24] Athans M. and Chang C., U.S. Department of Commerce Technical Report A, **ESD-TR-76-184** (1976).

[25] Palmer T. and Shukla J., *Q. J. R. Meterol. Soc.*, **126** (2000) 1989.

[26] Hagedorn R., Doblas-Reyes F. and Palmer T., *Tellus A*, **57** (2005) 219.

[27] Zhang S., Li D. and Qiu C., *Adv. Atmos. Sci.*, **28** (2010) 195.

[28] Hodgkin A. and Huxley A., *J. Physiol.*, **117** (1952) 500.

[29] Hindmarsh J. and Rose R., *Proc. R. Soc.*, **221** (1984) 87.

[30] Hamilton F., Berry T., Peixoto N. and Sauer T., *Phys. Rev. E*, **88** (2013) 052715.

[31] Cressman J., Ullah G., Ziburkus J., Schiff S. and Barreto E., *J. Comput. Neurosci.*, **26** (2009) 159.

[32] Knaack G., Charkhkar H., Hamilton F., Peixoto N., O'Shaughnessy T. and Pancrazio J., *NeuroToxicology*, **37** (2013) 19.

[33] Jensen M. and Yaari Y., *J. Neurophysiol.*, **77** (1997) 1124.

[34] Simon D., *Optimal State Estimation: Kalman, H_∞, and Nonlinear Approaches* (John Wiley and Sons) 2006.